IEEE Access
Multidisciplinary | Rapid Review | Open Access Journal

Received August 24, 2016, accepted September 5, 2016, date of publication October 19, 2016, date of current version November 8, 2016.

Digital Object Identifier 10.1109/ACCESS.2016.2616383

Power and Rate Adaptation Based on CSI and Velocity Variation for OFDM Systems Under Doubly Selective Fading Channels

ZHI-CHENG DONG[1,2], (Member, IEEE), PING-ZHI FAN[1], (Fellow, IEEE), XIAN-FU LEI[1], (Member, IEEE), AND ERDAL-PANAYIRCI[3], (Life Fellow, IEEE)

[1]Key Laboratory of Info Coding & Transmission, Southwest Jiaotong University, Chengdu 610031, China
[2]School of Engineering, Tibet University, Lhasa 850000, China
[3]Department of Electrical and Electronics Engineering, Kadir Has University, Istanbul 34230, Turkey

Corresponding author: Z. Dong (dongzc666@163.com)

This work was supported in part by the National Basic Research Program of China (973 Program) under Grant 2012CB316100, in part by the National Science Foundation of China under Grant 61561046, in part by the 111 Project under Grant 111-2-14, in part by the Fundamental Research Funds for the Central Universities under Grant SWJTU12ZT02/2682014ZT11, in part by the Key Project of Science Foundation of Tibet Autonomous Region under Grant 2015ZR-14-3, in part by the 2015 Outstanding Youth Scholars of Everest Scholars Talent Development Support Program of Tibet University.

ABSTRACT In this paper, a novel joint continuous power and rate adaptation scheme is proposed for doubly selective fading channels in orthogonal frequency division multiplexing (OFDM) systems, based on terminal velocity and perfect or imperfect channel state information (CSI). The analysis and simulation results show that the continuous power and rate adaptation scheme is very effective and improve the performance of OFDM systems substantially under time-varying fading channels, as compared with the traditional adaptation schemes operating without *a priori* knowledge of velocity and mobility adaptation without CSI.

INDEX TERMS OFDM, time-varying fading channels, average spectral efficiency, velocity variation, inter-carrier interference.

I. INTRODUCTION

OFDM has become an important transmission technique [1], because of its impeccable ability to counteract the inter-symbol interference (ISI) resulted from the frequency selective fading channels. Many wireless communication standards have adopted OFDM scheme, such as the IEEE 802.16 family (WiMAX) and the Third-Generation Partnership Project (3GPP) in the form of its long-term evolution (LTE) project. However, OFDM is sensitive to the inter-carrier interference (ICI) when the loss of orthogonality among subchannels is destroyed under the rapidly varying time-selective fading channels, causing the performance of OFDM systems to be sharply deteriorated, [2], [3].

Adaptive transmission is an effective technique to improve system performance [4]–[7]. In [4], the authors proposed a variable-rate and variable-power adaptive transmission method based on CSI. The authors proposed a multiobjective optimization for the bit and power allocation problem based on CSI in [5]. Adaptive techniques are widely employed in 3G (third-generation), such as high-speed downlink packet access (HSDPA) and high speed uplink packet access (HSUPA) [6]. Even for a promising candidate as a new multiple access scheme for future radio access, the adaptation is also very important to improve the system performance [7].

Adaptive techniques can also be employed to improve the performance of OFDM systems under fast time-varying channels because of its effect on reducing the impact of ICI. Many researchers have concluded that adjusting the system parameters (bit rate, transmit power, subcarrier bandwidth, etc.) based on the instantaneous CSI is effective under average power and instantaneous bit error rate (BER) constraints [8]–[13]. In [8] and [9], the authors investigated the power and rate allocation based on imperfect and perfect CSI. The authors in [10] investigated the subcarrier and rate allocation based on perfect CSI. In [11], a subcarrier bandwidth, power and rate adaptation based on perfect CSI are also proposed. On the other hand, the main cause of the ICI in OFDM-based systems is high mobility due to the rapidly moving terminals connected to the system [2], [3], [8]. It is well known that the ICI is directly proportional to the terminal velocities and the system performance degrades substantially

as the channel rapidly changes due to high mobilities of terminals [10]. For systems whose velocities change rapidly in time, velocity variations can be taken into account to improve the spectral efficiency as well as the system performance based on the instantaneous velocity and its probability distribution [13], similar to the traditional adaptation schemes based only on CSI. Consequently, as the adaptation algorithm allocates more power to lower velocities, it tends to allocate less power to larger velocities under the assumed power constraints. To the best of our knowledge, the mobility adaptation[1] based on the use of velocity variations has not been considered in the above references before. However, a subcarrier bandwidth and rate adaptation scheme based only on velocity has been studied in [12] and in [13], the authors studied the power adaptation based only on instantaneous velocity and the prior knowledge of velocity. The CSI, although not accurate under high mobility scenarios, is normally available with the help of pilot symbols. But CSI is not utilized at all in [12] and [13]. In this paper, we propose a new continuous power and rate[2] adaptation scheme for OFDM systems over fast fading channels that adjusts the transmit power and the rate based on both terminal velocities and the perfect or imperfect CSI in OFDM systems. The proposed scheme makes use of the complete knowledge of the velocity and the perfect or imperfect channel gains. Hence, the adaptation can utilize the advantage of channel and velocity variations jointly. Computer simulation results show that the proposed adaptation scheme is very effective for OFDM systems in the presence of time-varying channels, as compared with a traditional adaptation scheme that does not use the prior knowledge of the velocity [8] and mobility adaptation that does not use CSI [13]. If the velocity of a terminal is low,[3] performance of the proposed adaptation is close to the traditional adaptation. If the velocity of terminal is high, the performance of proposed adaptation is close to mobility adaptation. However, if the velocity of terminal stay an intermediate level, the proposed adaptation based on velocity and imperfect CSI should be employed.

The rest of the paper is organized as follows. The system model is introduced in Section II. The adaptation based on mobility and perfect CSI is presented in Section III while the adaptation based on mobility and imperfect CSI is investigated in Section IV. Some typical simulation results and discussions are provided in Section V. Finally, Section VI concludes this work.

[1]It is a new kind of adaptation based on the terminal velocity instead of CSI [12], [13].

[2]In practical system, the constellation point must be an integer number. The real-valued continuous constellation size can be truncated to the nearest integer practical value.

[3]In this paper, the velocity is a variable and a truncated normal probability distribution is adopted to model the velocity variations. The probability that a terminal velocity falls in a given velocity range is different for different parameter settings. In this paper, the mean $\mu \geq 200$ km/h denotes high velocity. $100 \leq \mu < 200$ km/h means intermediate velocity and $0 \leq \mu < 100$ km/h presents low velocity.

II. SYSTEM MODEL

In this paper, particularly, a downlink transmission scenario for OFDM systems is considered in which the transmitter is a ground base station and the receiver is on the terminal vehicle. Both the CSI and the terminal velocity are assumed to be time-varying random quantities having certain probability distributions. Specifically, in real-life applications, the terminal velocity variations in time are quite slow as compared to the variations in wireless channel gains between the terminal and the base station. Thus, the terminal velocity is assumed to be constant during a data block consisting of a ceratin number of OFDM symbols but to change from data block to data block following a truncated normal distribution [14]. The transmitter (ground base station) obtains information about the channel state and terminal velocity to achieve power and rate adaptation. The velocity and the CSI can be estimated at the receiver using different techniques, such as those presented in [15]–[17] and then are fed back through a dedicated feedback channel [18] to the transmitter of the OFDM system for making handover and power as well as rate adaptations.

For an OFDM system, the discrete time-domain received signal at the input of the discrete Fourier transform (DFT) can be written as [19]

$$y(m) = \sum_{\ell=0}^{L-1} h(m, \ell)\, x(m-\ell) + w(m), \tag{1}$$

where $h(m, \ell)$ denotes the channel impulse response of the ℓth path at discrete-time m. The number of multipaths of time-varying channel is L. $w(n)$ is complex additive white Gaussian noise (AWGN) with mean zero and variance σ_w^2. The signal $x(m)$ is the time-domain transmitted signal at time m, which can be expressed as

$$x(m) = \frac{1}{\sqrt{K}} \sum_{n=0}^{N-1} d(n) e^{j2\pi mn/K}, \quad -L_{CP} \leq m \leq K-1, \tag{2}$$

where N is the number of useful subcarriers per OFDM symbol, K is the FFT size. $d(n)$ represents the data symbols generated from a set of multi-level signal constellations such as M-level quadrature amplitude modulation (MQAM) to be transmitted in the frequency domain over the nth OFDM subcarrier. L_{CP} denotes the number of cyclic prefix. It is assumed that the maximum number of multipaths of time-varying channel L is less than the number of cyclic prefix to eliminate the ISI. Also, the average transmitted signal power on each OFDM subcarrier is denoted by $\overline{S} = E\{|d(n)|^2\}$. The signal on the nth subcarrier in the frequency domain can be expressed as [19]

$$\begin{aligned} Y(n) &= \frac{1}{\sqrt{K}} \sum_{m=0}^{K-1} y(m)\, e^{-j2\pi mn/K} \\ &= d(n)H(n) + I(n) + W(n), \end{aligned} \tag{3}$$

where $I(n)$ denotes the ICI power, defined as $I(n) = 1/K \sum_{k=0,k\neq n}^{N-1} d(k) \sum_{m=0}^{K-1} H_k(m)\, e^{j2\pi m(k-n)/K}$,

$H(n) = (1/K)\sum_{m=0}^{K-1} H_n(m)$, $H_n(m)$, being the Fourier transform of the time-varying channel at time m for an OFDM system, defined as $H_n(m) = \sum_{\ell=0}^{L-1} h(m, \ell)\exp(-j2\pi\ell n/K)$, and $W(n) = \frac{1}{\sqrt{K}}\sum_{m=0}^{K-1} w(m)\exp(-j2\pi mn/K)$.

Assuming the L-path time-varying channel is modeled as a wide-sense stationary uncorrelated scattering Rayleigh fading channel, the autocorrelation of the channel frequency response $H_n(m)$, at discrete time n, can be determined for

$$E\{H_n(m)H_n^*(m')\} = J_0\left(2\pi f_{\max} T_{\text{OFDM}}(m-m')/K\right),$$

where J_0 is the zeroth-order Bessel function of the first kind [19]. T_{OFDM} represents the OFDM symbol duration, defined as $T_{\text{OFDM}} = KT_s + L_{CP}T_s$, T_s being the sampling duration. The maximum Doppler frequency, $f_{\max}$, is defined as $f_{max} = f_c v/c$, where f_c is the carrier frequency, v is the terminal velocity in [km/h] during a data block period and c denotes the speed of light.

Since the ICI power, P_{ICI}, generated in each subcarrier is approximately independent of the subchannel index when the number of OFDM subcarriers is large [8], [19], it can be expressed as

$$P_{ICI} = E\{|I(n)|^2\} = P_N\overline{S}, \quad 0 \le n \le N-1. \tag{4}$$

where P_N denotes the normalized ICI power that can be determined from [2],

$$P_N \le \frac{\alpha_1}{12c^2}(2\pi f_c v T_{\text{OFDM}})^2 = \frac{1}{24c^2}(2\pi f_c v T_{\text{OFDM}})^2. \tag{5}$$

where $\alpha_1 = 1/2$ [2]. Note that, according to Eq. (5), P_N increases with velocity v, quadratically.

III. ADAPTATION BASED ON MOBILITY AND PERFECT CSI

It is easy to see from (4) that the ICI power at different subcarriers are approximately independent of the OFDM subcarrier indices when the number of subcarriers is large [8], [19], [20]. Consequently, the instantaneous effective signal to interference plus noise ratio (SINR) for the nth subcarrier of the OFDM system can be expressed as

$$SINR(n) = \frac{\overline{\gamma}|H_n|^2}{P_N\overline{\gamma}+1} = \frac{\gamma}{P_N\overline{\gamma}+1}, \tag{6}$$

where $\overline{\gamma} = \overline{S}/\sigma_w^2$ and $\gamma = \overline{\gamma}|H_n|^2$ denotes the instantaneous received SNR.

In most of the highly mobile real systems, such as high speed trains, the speed of vehicle is a time-varying random quantity. Mostly, a truncated normal probability distribution $\mathcal{N}(\mu, \sigma_v^2)$ is adopted to model the velocity variations in such systems [13], [14], where μ and σ_v^2 denote the mean and the variance of the variations, respectively. Probability density function (pdf) of the velocity, $f(v)$, can be expressed as [13], [14]

$$f(v) = \frac{2\exp\left(-\frac{(v-\mu)^2}{2\sigma_v^2}\right)}{\sigma_v\sqrt{(2\pi)}\left(\text{erf}\left(\frac{\sqrt{2}(v_{\max}-\mu)}{2\sigma_v}\right) - \text{erf}\left(\frac{\sqrt{2}(v_{\min}-\mu)}{2\sigma_v}\right)\right)}, \tag{7}$$

where erf(.) is the error function defined as $\text{erf}(x) = 2/\sqrt{2\pi}\int_0^x \exp(-t^2)dt$, $v_{\min}$ and $v_{\max}$ denote the minimum velocity and maximum velocity, respectively. If there is no special instructions, $v_{\min} = 0$ km/h and $v_{\max} = 300$ km/h in this paper.

In this paper, both the channel fading and the velocity are assumed to be time-varying quantities having some specific probability distributions. However, since the velocity varies much slower than the variations in channel gains, it is reasonable to assume that the terminal velocity is constant within the duration of a data block [13]. However, each data block consists of a large number of OFDM symbols which undergoes the greater effect of doubly-selective fading channels. Therefore, different subcarriers of an OFDM symbol experience different channel gains in the frequency domain. For adaptation schemes based on channel gains, it is very hard to evaluate the exact ICI. However, since time-varying channels produce a nearly-banded channel matrix, adjacent subcarriers have almost the same channel gains [17]. Also, it is assumed that the coherence bandwidth is large enough so that the channel coefficients are approximately the same for most of the significant (neighboring) subcarriers causing ICI [10].

Let $P(v, \gamma)$ denotes the power level allocated to each OFDM subchannel, as a function of the CSI γ and the velocity v. Then, the effective SINR for the nth subcarrier of the OFDM system can be expressed as [10]

$$SINR(n) = \frac{\gamma P(v,\gamma)}{P_N\overline{\gamma}P(v,\gamma)+1}. \tag{8}$$

We now present the details to obtain the optimal $P(v, \gamma)$ that maximizes the average spectral efficiency (C_{ASE}) in bits/sec/Hz. It is obvious that $P(v, \gamma)$ is determined with the help of the prior knowledge provided both by the terminal velocities and the channel gains as opposed to the traditional adaptation schemes where only the knowledge of channel gains would be sufficient [4], [8], [21]. Consequently first time in the literature, in this work, the power and rate are adjusted on each OFDM subcarrier based on the terminal speeds as well the channel variations. The resulting novel adaptation scheme have potential applications for high mobility wireless communications systems.

Based on (8), the BER can be bounded as [4], [8]–[11], [20], [22]

$$\Omega \le C_1\exp\left(\frac{-C_2\gamma P(v,\gamma)}{\left(2^{R(v,\gamma)}-1\right)\left(P_N\overline{\gamma}P(v,\gamma)+1\right)}\right), \tag{9}$$

where $C_1 = 0.2$, $C_2 = 1.5$, $\gamma = \overline{\gamma}|H(n)|^2$, and $R(v, \gamma)$ is the data rate in bits/sec for any subcarrier with channel gain γ and during a data block with velocity v. Using the upper bound for BER according to (9), the maximum $R(v, \gamma)$ can be obtained easily as follows.

$$R(v,\gamma) = \log_2\left(\frac{\xi\gamma P(v,\gamma)}{P_N\overline{\gamma}P(v,\gamma)+1}+1\right), \tag{10}$$

where $\xi = -C_2/\log(C_3/C_1) = -1.5/\log(5C_3)$ and C_3 is the target BER.

The average spectral efficiency, C_{ASE} can be obtained by simply averaging $R(v,\gamma)$ over the probability distributions of velocity v and channel gain γ as follows

$$C_{ASE} = \xi \int_{v_{\min}}^{v_{\max}} \int_0^{\infty} \log_2\left[\frac{\xi\gamma P(v,\gamma)}{P_N\overline{\gamma}P(v,\gamma)+1}+1\right] p_\gamma(\gamma) f(v) d\gamma dv, \quad (11)$$

where $\xi = \frac{N}{(N+L_{CP})\Delta f T_{OFDM}}$, $p_\gamma(\gamma) = 1/(\overline{\gamma}\rho)\exp(-\gamma/(\overline{\gamma}\rho))$ [2], [8], [19] and Δf is subcarrier spacing in Hz for an OFDM system.

To maximize C_{ASE}, the following constrained optimization problem is formulated as

$$\max_{P(v,\gamma)} \int_{v_{\min}}^{v_{\max}} \int_0^{\infty} \log_2\left[\frac{\xi\gamma P(v,\gamma)}{P_N\overline{\gamma}P(v,\gamma)+1}+1\right] \times p_\gamma(\gamma) f(v) d\gamma dv \quad (12a)$$

subject to

$$\int_{v_{\min}}^{v_{\max}} \int_0^{\infty} P(v,\gamma) p_\gamma(\gamma) f(v) d\gamma dv = 1, \quad (12b)$$

$$P(v,\gamma) \geq 0, \quad (12c)$$

where the constraints (12b) and (12c) indicate that the power allocation based on CSI γ and the velocity v must meet the average power constraint and that the power allocation based on CSI γ and the velocity v must be positive quantities, respectively.

In Appendices A and B, it is proved that Eq. (12a) is concave with respect to $P(v,\gamma)$ and that Eq. (12b) is affine, respectively. It is then straightforward to show that Eq. (12c) is convex with respect to $P(v,\gamma)$. Hence, the optimal solution can be obtained easily by the *Karush-Kuhn-Tucker* (KKT) conditions.

We define the Lagrangian for the optimization problem as in (13), as shown at the bottom of this page, where λ is Lagrange multipliers for the equality constraints, and ϑ is multiplier for the inequality constraint.

In Appendix C, it is proved that ϑ acts as a slack variable and it can be eliminated. Consequently, the equality condition along with elimination of the slack variable yields the optimal λ^* and $P^*(v,\gamma)$ that can be obtained by the optimization formulation in (14), as shown at the bottom of this page [23], where λ is a Lagrangian constant and there is no closed form solution for it. However, it can be computed easily through a numerical search[4] [4].

The optimal power adaptation, based on channel gain γ and velocity v, can be obtained by solving the equation $\frac{\partial L_a\{P(v,\gamma)\}}{\partial P(v,\gamma)} = 0$ to yield

$$P(v,\gamma) = \frac{-2\ln(2)\lambda P_N\overline{\gamma} - \ln(2)\lambda\xi\gamma + \sqrt{C_5}}{2\ln(2)\lambda P_N\overline{\gamma}\,(P_N\overline{\gamma}+\xi\gamma)}, \quad (15)$$

where $C_5 = \ln(2)\lambda\xi\gamma\left(\ln(2)\lambda\xi\gamma + 4\gamma\xi P_N\overline{\gamma} + 4\overline{\gamma}^2P_N^2\right)$. Taking the upper bound of normalized ICI power $\frac{1}{24c^2}(2\pi f_c v T_{\mathrm{OFDM}})^2$ in (5) equal to P_N, the optimal power distribution in (15) is a two dimension joint scheme based on velocity v and CSI gain γ. It can be seen that when $P(v,\gamma) \geq 0$, there exists a cutoff $\gamma_{off} = \frac{\ln(2)\lambda}{\xi}$, below which no data is transmitted.

According to the velocity v and channel gain γ, the corresponding optimal rate adaptation can be expressed from (10) as,

$$R(v,\gamma) = \max\left\{0, \log_2\left[\frac{-\left(\ln(2)\lambda\xi\gamma - \sqrt{C_5}\right)(P_N\overline{\gamma}+\xi\gamma)}{\left(\ln(2)\lambda\xi\gamma + \sqrt{C_5}\right)P_N\overline{\gamma}}\right]\right\}, \quad (16)$$

where $P_N = \frac{1}{24c^2}(2\pi f_c v T_{\mathrm{OFDM}})^2$ is the upper bound in (5). It can be seen from (16) that the optimal rate distribution is also a two dimensional joint scheme based on velocity v and CSI gain γ.

The adaptive algorithm based on mobility and perfect CSI is implemented by the following steps.

1. Estimate the mobile terminal velocity v and perfect channel gain γ.
2. Achieve the optimal power $P^*(v,\gamma)$ according to Eq. 15.
3. Achieve the optimal rate $R^*(v,\gamma)$ according to Eq. 16.

IV. ADAPTATION BASED ON MOBILITY AND IMPERFECT CSI

In a real wireless communication system, it is impossible to obtain perfect CSI due to error-prone channel estimation and an unavoidable delay between channel estimation and

[4]Substitute power distribution $P(v,\gamma)$ in (15) into (12b), then get λ by solving equation (12b). Since there is no closed form expression for the integral of (12b), we cannot obtain a closed form expression for λ. However, we can solve numerically using fsolve command of Maple [24].

$$L_a\{P(v,\gamma)\} = \int_{v_{\min}}^{v_{\max}} \int_0^{\infty} \log_2\left[\frac{\xi\gamma P(v,\gamma)}{P_N\overline{\gamma}P(v,\gamma)+1}+1\right] p_\gamma(\gamma) f(v) d\gamma dv - \lambda\left(\int_{v_{\min}}^{v_{\max}} \int_0^{\infty} P(v,\gamma) p_\gamma(\gamma) f(v) d\gamma dv - 1\right) - \vartheta P(v,\gamma). \quad (13)$$

$$L_a\{P(v,\gamma)\} = \int_{v_{\min}}^{v_{\max}} \int_0^{\infty} \log_2\left[\frac{\xi\gamma P(v,\gamma)}{P_N\overline{\gamma}P(v,\gamma)+1}+1\right] p_\gamma(\gamma) f(v) d\gamma dv - \lambda\left(\int_{v_{\min}}^{v_{\max}} \int_0^{\infty} P(v,\gamma) p_\gamma(\gamma) f(v) d\gamma dv - 1\right). \quad (14)$$

feedback to the transmitter for actual transmission [25], [26]. We now extend the results obtained in previous section to the case in which the adaptation based on mobility is achieved in the presence of imperfect CSI.

The channel estimator at the receiver provides the transmitter with an imperfect CSI, $H_k'(n+\Delta n)$, which is assumed to be in the form $H_k'(n+\Delta n) = H_k(n+\Delta n) + \epsilon_k(n)$, where $\Delta n = \lceil \tau_D / T_{OFDM} \rceil$ is an integer-valued delay, greater than zero, between channel estimation at the receiver at time nT_s and using the estimation result at the transmitter at time $nT_s + \Delta n T_{OFDM}$ [27]. τ_D denotes the unavoidable delay between the channel estimation at the receiver and using at the transmitter. The channel estimation error, denoted by $\epsilon_k(n)$, is independent of the actual channel gain $H_k(n)$ and is distributed according to $\mathcal{CN}(0, \sigma_p^2)$ [28]. For the sake of analysis, we assume that σ_p^2 and Δn are statistically independent.

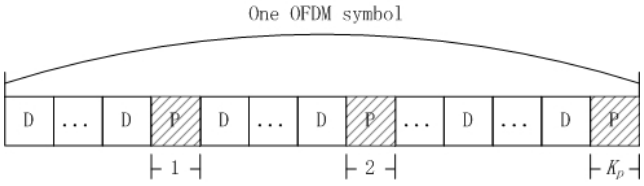

FIGURE 1. Insertion of pilots in frequency domain for an OFDM symbol.

Equally spaced piloted symbols are inserted in the OFDM subcarriers for channel estimation, as is shown in Fig. 1, where P and D denote the pilot and data symbols, respectively. We employ a pilot-aided minimum mean squared error (MMSE) channel estimation technique that results in a mean square error (MSE) σ_p^2 given by [29]

$$\sigma_p^2 = \frac{1}{K_p}\text{trace}(\mathbf{R}_{ee}), \tag{17}$$

where K_p is the number of pilot symbols and $\delta = K_p/N$ is the percentage of pilot symbols in one OFDM symbol [29]. If there is no special instructions, we assume $\delta = 1/10$ and $K_p = \text{ceil}(N \times \delta)$ in this paper, where ceil(x) denotes the smallest integer bigger than or equal to x. The correlation matrix of the error vector, $\mathbf{R}_{ee}$, can be calculated as [29]

$$\mathbf{R}_{ee} = \mathbf{R}_{PP} - \mathbf{R}_{DP}\left(\mathbf{R}_{PP} + \frac{1}{\gamma_P}\mathbf{I}_{K_p}\right)^{-1}\mathbf{R}_{DP}^H, \tag{18}$$

where $\gamma_P = \frac{\overline{\gamma}(1-P_N)}{\overline{\gamma}P_N+1}$, which is the average effective SINR.[5] and $\mathbf{R}_{PP} = r_t(0)\mathbf{R}_f$, where $r_t(0) = 1/K^2 \sum_{m_1=0}^{N-1}\sum_{m_2=0}^{N-1} J_0\left(2\pi f_{\max} T_{\text{OFDM}}(m_1-m_2)/K\right)$ and $r_f(\Delta k) = c_a \sum_l \exp(-l/L)\exp(-j2\pi\Delta k l/K)$, where c_a, is a normalization constant, is chosen to satisfy $c_a \sum_l \exp(-l/L) = 1$ [19], as shown at the bottom of this page, and

$$\mathbf{R}_f = \begin{bmatrix} r_f(0) & r_f(-1/\delta) & \dots & r_f((-K_p+1)/\delta) \\ r_f(1/\delta) & r_f(0) & \dots & r_f((-K_p+2)\delta) \\ \vdots & \vdots & \dots & \vdots \\ r_f((K_p-1)/\delta) & r_f((K_p-2)/\delta) & \dots & r_f(0) \end{bmatrix}.$$

The cross-correlation matrix, $\mathbf{R}_{DP} \in \mathcal{R}^{K_p \times K_p}$, in (18) is a Toeplitz matrix with its first row being $[r_t(0)r_f(-1/\delta+u), r_t(0)r_f(-2/\delta+u), \cdots, r_t(0)r_f(-K_p/\delta+u)]$ and the first column is $[r_t(0)r_f(-1/\delta+u), r_t(0)r_f(u), \cdots, r_t(0)r_f((K_p-2)/\delta+u)]$. $\mathbf{I}_{K_p}$ is $K_p \times K_p$ identity matrix. Hence, σ_p^2 is a function of the velocity v, the percentage of the pilot symbols δ and the average pilot transmission power $\overline{\gamma}$.

The correlation between H_k and H_k' can be expressed as in (19) [27].

Due to the fact that $f_{\max} = f_c v/c$, the correlation r is a function of velocity v.

Assume now that for $k = 0, 1, \cdots, K-1$, H_k' is the only CSI perfectly known by the OFDM kth subcarrier at the transmitter. Since the instantaneous BER for each subcarrier $\Omega([k])$ is determined by the true value of CSI, $\gamma[k] = \overline{\gamma} \mid H_k \mid^2$, which is assumed unknown, it would not be possible to fix $\Omega([k])$ to be the BER requirement. However, we can define a conditional average BER given H_k'. The instantaneous BER of each subcarrier, considering both channel estimation error and outdated CSI, can be obtained as [27]

$$\Omega([k]) \le C_1 \exp\left[\frac{-C_2\gamma P'(v,\gamma)}{\left(2^{R'(v,\gamma)}-1\right)(\phi P'(v,\gamma)+1)}\right], \tag{20}$$

where $\phi = P_N\overline{\gamma} + \overline{\gamma}(N-1)\sigma_p^2/N$ [8], [27].

[5]The authors did not consider the impact of ICI on system performance in [29]. However, the impact of ICI cannot be ignored for OFDM under fast fading channels. Hence, the ICI power is modeled as a Gaussian noise in this paper, having the average ICI power equals to $\overline{\gamma}P_N$.

$$r = E\{H_k^\dagger H_k'\} = \frac{NJ_0}{K^2}\left(\frac{2\pi f_{\max} T_{sys}\Delta n}{K}\right) + \frac{1}{K^2}\sum_{n=1}^{N-1}(N-n)J_0\left(\frac{2\pi f_{\max} T_{OFDM}(n+\Delta n)}{K}\right) + \frac{1}{K^2}\sum_{n=1}^{N-1}(N-n)J_0\left(\frac{2\pi f_{\max} T_{OFDM}(n-\Delta n)}{K}\right). \tag{19}$$

$$\overline{\Omega}([k]) \leq \int_0^{\infty} C_1 \exp\left[\frac{-C_2 z^2 \overline{\gamma} P'(v,\gamma')}{\left(2^{R'(v,\gamma')}-1\right)(\phi P'(v,\gamma')+1)}\right] \frac{2z}{\sigma^2} \exp\left\{-\frac{z^2+|\mu|^2}{\sigma^2}\right\} I_0\left(\frac{2z|\mu|}{\sigma^2}\right) dz$$
$$= \frac{C_1\left(\phi P'(v,\gamma')+1\right)\left(2^{R'(v,\gamma')}-1\right) \exp\left(-\frac{C_2|\mu|^2\overline{\gamma}P'(v,\gamma')}{C_2\overline{\gamma}\sigma^2 P'(v,\gamma')+\left(2^{R'(v,\gamma')}-1\right)(\phi P'(v,\gamma')+1)}\right)}{C_2\overline{\gamma}\sigma^2 P'(v,\gamma')+\left(2^{R'(v,\gamma')}-1\right)(\phi P'(v,\gamma')+1)} \quad (21)$$

For the special case when the probability distribution of H_k given H_k' is a complex Gaussian with mean μ and variance σ^2 [8], [20], it follows that $z = |H_k|$ conditioned on H_k' is a Rician distribution [20]. Based on (20), the average BER for the kth subchannel is defined as $\overline{\Omega}([k]) = E_{z|H_k'}\{\Omega([k])\}$, as shown in (21), as shown at the top of this next page, where $I_0(\cdot)$ denotes the zeroth-order modified Bessel function of the first kind.

Using the Gaussian assumption, it can be shown that H_k given $H_k{}'$ is a Gaussian distribution with mean [20], [27]

$$u = \frac{r}{\rho_0 + \sigma_p^2/N} H_k', \quad (22)$$

and variance

$$\sigma^2 = \rho_0 - \frac{r^2}{\rho_0 + \sigma_p^2/N}. \quad (23)$$

where ρ_0 denotes the correlation between H_k and $H_k{}'$ when there is no delay ($\Delta n = 0$) between the channel estimation performed at the receiver and the time using this estimate at the transmitter. That is $\rho_0 = r$ with $\Delta n = 0$ in (19). Consequently, the above mean and variance expressions take the forms, $u = \frac{\rho_0}{\rho_0+\sigma_p^2/N} H_k'$ and variance $\sigma^2 = \frac{\rho_0(\sigma_p^2/N)}{\rho_0+\sigma_p^2/N}$ [8], respectively. On the other hand, if there is no estimation error, $\sigma_p^2 = 0$, H_k given $H_k{}'$ has mean $u = (r/\rho_0)H_k'$ and variance $\sigma^2 = \rho_0 - r^2/\rho_0$ [8].

Assume now that $\overline{\Omega}([k]) = C_3$, where C_3 is the target BER. Using the upper bound for the average BER given by (21), the maximum $R'(v,\gamma')$ can be expressed as in (24), as shown at the bottom of this page, where $B_1 = r^2\gamma'/\left(\rho_0 + \sigma_p^2/N\right)^2 \overline{\gamma}$, $B_3 = B_1 C_3 \exp\left(B_1/\sigma^2\right)/C_1\sigma^2$, $B_4 = C_2\overline{\gamma}\sigma^4$ and $W(.)$ denotes the Lambert W-function that satisfies $W(x)\exp(W(x)) = x$, as shown in [30]. B_1 and B_3 are functions of v and γ'.

The average spectral efficiency, in the presence of the imperfect CSI, C'_{ASE}, can be obtained by simply averaging $R'(v,\gamma')$ over the probability distributions of velocity v and channel gain γ' in (25), as show at the bottom of this page, where $p_{\gamma'}(\gamma') = 1/(\overline{\gamma}\rho)\exp(-\gamma'/(\overline{\gamma}\rho))$ [8], [13], [27].

To maximize C'_{ASE}, the following constrained optimization problem is formulated as in (26a), (26b) and (26c), as shown at the bottom of this page.

In Appendix D, it is proved that Eq. (26a) is concave with respect to $P'(v,\gamma')$. It is then straightforward to show that Eq. (26b) and Eq. (26c) are convex with respect to $P'(v,\gamma')$. Similarly, we can also show in Appendix B that Eq. (26b) is affine. Hence, the optimal solution can be obtained easily by the KKT conditions.

The Lagrangian for the optimization problem can be written as in (27), as show at the top of the next page,

$$R'(v,\gamma') = \log_2\left(\frac{B_1\left(\phi P'(v,\gamma')+1\right)+B_4 P'(v,\gamma')W(B_3)-\sigma^2 W(B_3)\left(\phi P'(v,\gamma')+1\right)}{\left(B_1-\sigma^2 W(B_3)\right)\left(\phi P'(v,\gamma')+1\right)}\right) \quad (24)$$

$$C'_{ASE} = \frac{N-K_p}{(N+L_{CP})\Delta f T_{OFDM}} \int_{v_{\min}}^{v_{\max}} \int_0^{\infty} \log_2\left[\frac{B_1\left(\phi P'(v,\gamma')+1\right)+B_4 P'(v,\gamma')W(B_3)-\sigma^2 W(B_3)\left(\phi P'(v,\gamma')+1\right)}{\left(B_1-\sigma^2 W(B_3)\right)\left(\phi P'(v,\gamma')+1\right)}\right]$$
$$p_{\gamma'}(\gamma') f(v) d\gamma' dv, \quad (25)$$

$$\max_{P(v,\gamma')} \int_{v_{\min}}^{v_{\max}} \int_0^{\infty} \log_2\left[\frac{B_1\left(\phi P'(v,\gamma')+1\right)+B_4 P'(v,\gamma')W(B_3)-\sigma^2 W(B_3)\left(\phi P'(v,\gamma')+1\right)}{\left(B_1-\sigma^2 W(B_3)\right)\left(\phi P'(v,\gamma')+1\right)}\right] p_{\gamma'}(\gamma') f(v) d\gamma' dv \quad (26a)$$

subject to

$$\int_{v_{\min}}^{v_{\max}} \int_0^{\infty} P'(v,\gamma') p_{\gamma'}(\gamma') f(v) d\gamma' dv = 1 \quad (26b)$$

$$P'(v,\gamma') \geq 0 \quad (26c)$$

$$L_a'\{P'(v,\gamma')\} = \int_{v_{\min}}^{v_{\max}} \int_0^{\infty} \log_2 \left[\frac{B_1\left(\phi P'\left(v,\gamma'\right)+1\right)+B_4 P'\left(v,\gamma'\right) W\left(B_3\right)-\sigma^2 W\left(B_3\right)\left(\phi P'\left(v,\gamma'\right)+1\right)}{\left(B_1-\sigma^2 W\left(B_3\right)\right)\left(\phi P'\left(v,\gamma'\right)+1\right)} \right]$$
$$\times p_{\gamma'}\left(\gamma'\right) f(v) d\gamma' dv - \lambda' \left(\int_{v_{\min}}^{v_{\max}} \int_0^{\infty} P(v,\gamma') p_{\gamma'}\left(\gamma'\right) f(v) d\gamma' dv - 1 \right), \tag{27}$$

$$P'(v,\gamma') = \frac{2\ln(2)\lambda'\sigma^2 W\left(B_3\right)\phi - \ln(2)\lambda' B_4 W\left(B_3\right) - 2\ln(2)\lambda' B_1\phi + \sqrt{C_6}}{2\ln(2)\lambda'\phi\left(B_1\phi + B_4 W\left(B_3\right) - \sigma^2 W\left(B_3\right)\phi\right)}, \tag{28}$$

$$R'(v,\gamma') = \max\left\{0, \log_2\left[\frac{\left(\sigma^2 W\left(B_3\right)\phi - B_1\phi - B_4 W\left(B_3\right)\right)\left(\lambda'\ln(2) B_4 W\left(B_3\right) - \sqrt{C_6}\right)}{\left(\lambda'\ln(2) B_4 W\left(B_3\right) + \sqrt{C_6}\right)\left(B_1 - \sigma^2 W\left(B_3\right)\right)\phi}\right]\right\}. \tag{29}$$

where λ' is the Lagrangian constant. Based on $\frac{\partial L_a'\{P'(v,\gamma')\}}{\partial P'(v,\gamma')} = 0$, the optimal power adaptation based on channel gain γ' and velocity v can be obtained as in (28), as shown at the top of this page, where $C_6 = (\ln(2)\lambda' B_4 W(B_3) + 4\phi^2 B_1 + 4\phi B_4 W(B_3) - 4\phi^2\sigma^2 W(B_3))\ln(2)\lambda' B_4 W(B_3)$. C_6 is a function of v and γ' based on (24).

As in the perfect CSI case, there is no closed form expressions to evaluate λ'. However, it can be computed easily through a numerical search [4]. From Eq. (28) it can be seen that when $P'(v,\gamma') \geq 0$, there exists a cutoff value

$$\gamma'_{off} = \frac{\ln\left(\frac{C_1\sigma^2\lambda'\ln(2)}{(B_4+\lambda'\ln(2)\sigma^2)C_3}\right)\sigma^2\left(B_4+\lambda'\ln(2)\sigma^2\right)}{B_4 B_5},$$

below which no data is transmitted. Here, $B_5 = r^2/\left(\rho_0 + \sigma_p^2/N\right)^2\overline{\gamma}$. The optimal power distribution in (28) is a two dimension scheme based on velocity v and imperfect CSI gain γ', which consider the channel estimation error with MMSE and feedback delay.

According to the velocity v and channel gain γ, the corresponding optimal rate adaptation can be expressed as in (29), as shown at the top of this page,. The optimal rate distribution in (29) is also a two dimensional joint scheme based on velocity v and imperfect CSI gain γ', that yields channel estimation errors when employed with a MMSE channel estimation technique and in the presence of a feedback delay.

The adaptive algorithm proceeds based on mobility and imperfect CSI is implemented as follows.

1. Estimate the mobile terminal velocity v.
2. Estimate the imperfect channel gain γ' based on MMSE channel estimation technique with the percentage of pilot symbols δ in one OFDM symbol.
3. Achieve the optimal power $P^*(v,\gamma')$ according to Eq. 28.
4. Achieve the optimal rate $R^*(v,\gamma')$ according to Eq. 29.

V. SIMULATION RESULTS

We now present some computer simulation results to analyze and verify the proposed adaptation scheme based on mobility and CSI. In all simulations presented here, the OFDM system parameters are given in Table I according to LTE specifications [31]. Each coefficient of the time-domain channel impulse response is considered as Rayleigh distributed with Jakes' spectrum. Exponential power delay profile with maximum delay spread of $7.42\mu s$ is chosen and the required BER is assumed to be 10^{-3}. The proposed scheme is compared with traditional adaptation schemes without taking into account the prior knowledge of the velocity [8][6] with mobility adaptation schemes and without CSI [13].

TABLE 1. OFDM parameters [31].

FFT size (points) K	512
OFDM sampling rate (Msamples/sec) $1/T_s$	7.68
Guard time interval (cyclic prefix) L_{CP} (samples/μsec)	57/7.42
Subcarrier separation (KHz) Δf	15
OFDM symbol duration (μsec) T_{OFDM}	74.09
Number of useful subcarriers per OFDM symbol N	299
OFDM bandwidth(MHz) B	4.485
Carrier frequency of system (GHz) f_c	2

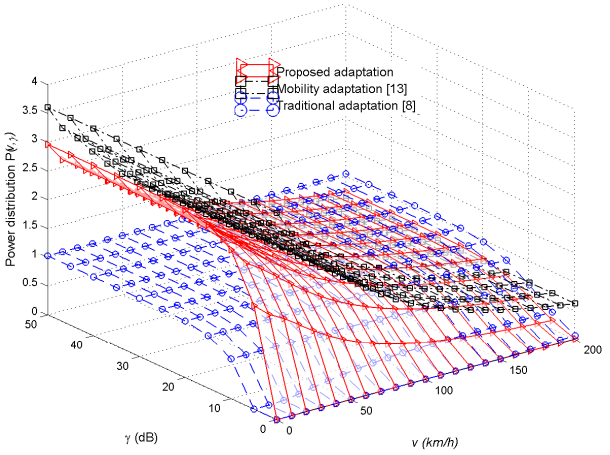

FIGURE 2. The power distribution vs. velocity v and channel gain γ (μ = 150 km/h, σ_v^2 = 45 km/h, SNR = 15 dB).

Fig. 2 shows the optimal power adaptation with $\overline{\gamma}$ = 15 dB and μ = 150 km/h, σ_v^2 = 45 km/h^2, as a function of the terminal velocity v and the channel gain γ. This figure clearly indicates that the power adaptation $P(v,\gamma)$

[6]In [8], the authors considered the impact of channel estimation error and delay on the system performance, separately. In order to compare the performance with the proposed scheme in this paper, the impact of channel estimation errors and delay on the system performance is considered jointly

increases monotonically with γ when v is fixed. However, it has a different behavior as a function of v when γ is kept fixed. That is, the power allocation will decrease toward zero monotonically as v increases. On the other hand, for traditional power adaptation schemes in which the prior knowledge of velocity is not taken into account, [8], the average transmission power is the same for all velocities v. For mobility adaptation schemes in which the knowledge of CSI is not taken into account, [13], the average transmission power is the same for all channel gain γ. Consequently, compared with the traditional and mobility adaptation, it is clear that the proposed power adaptation with prior knowledge of velocity and CSI will improve the performance of the system. More power will be allocated to the larger channel gains and lower velocities since the wireless channel is better and the ICI is smaller. We can see from Fig. 2 that the proposed power adaptation scheme will allocate largest power and largest channel gain in the vicinity of the lowest velocity region while it allocates smallest power vice versa. This means that lower velocity and larger channel gain play an important role in determining the overall system performance since the ICI in this region is low and the wireless channel is good. However, the traditional adaptation scheme and mobility adaptation do not have this trend.

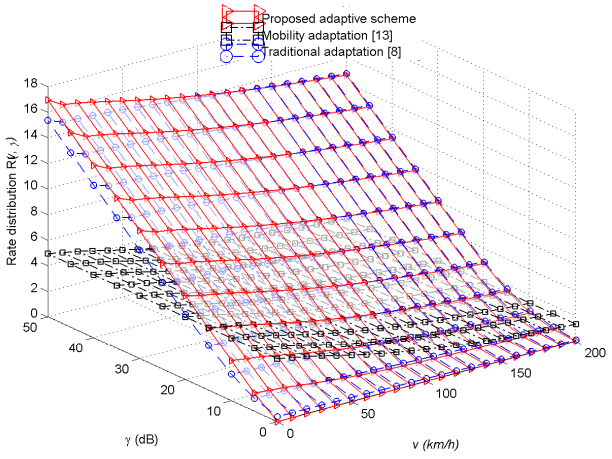

FIGURE 3. The rate distribution vs. velocity v and channel gain γ ($\mu = 150$ km/h, $\sigma_v^2 = 45$ (km/h)^2, SNR = 15 dB).

Fig. 3 shows the optimal rate adaptation with $\overline{\gamma} = 15$ dB and $\mu = 150$ km/h, $\sigma_v^2 = 45$ km/h^2, as a function of the terminal velocity v and the channel gain γ. In another words, the rate adaptation scheme, $R(v, \gamma)$, assigns higher bit rates monotonically as the channel gain γ increases and the velocity v is kept fixed. It can also be observed from the same figure that the rate adaptation behaves in an opposite way as v increases with γ is fixed. Besides the above conclusions, we also observe that at lower terminal velocities and larger channel gains, the proposed optimal rate adaptation scheme assigns larger bit rates than the traditional rate adaptation and mobility adaptation. However, similar to the above case, our optimal rate adaptation assigns smaller bit rates than the traditional adaptation and mobility adaptation, under larger velocities and lower channel gain. This implies that the proposed scheme improves the system performance by increasing the bit rate at lower velocities and larger channel gain, while reducing the effect of worse case in which larger velocities and lower channel gains are encountered by means of the power constraint.

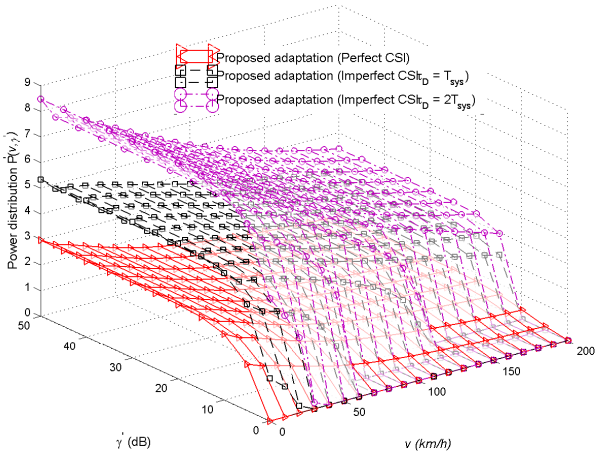

FIGURE 4. The power distribution vs. velocity v and channel gain γ' under imperfect CSI case ($\mu = 150$ km/h, $\sigma_v^2 = 45$ (km/h)^2, SNR = 15 dB).

In Fig. 4, the power allocation $P'(v, \gamma')$ is plotted as a function of the velocity and channel gain under imperfect CSI. It can be seen that there exists a cutoff velocity above and channel gain below which no power will be allocated at the transmitter. The lower velocity and larger channel gain region play an important role in determining the overall system performance since the ICI in this region is low and channel is good. From Fig. 4, one can see that imperfect CSI has significant influence on the power allocation. More specifically, it is obvious that more power should allocated to the low velocity and larger channel gain region as the delay Δn increases since the the system has less chance to work in this region. However, the power is lower in larger velocities and lower channel gain region because of the power constraint.

In Fig. 5, the corresponding rate adaptation $R'(v, \gamma')$ is illustrated as a function of the velocity and channel gain under imperfect CSI. It is shown that data rate decreases as the velocity increases. Again, the low velocity and large channel gain region determines the overall system performance. The data rate is higher in the lower velocity and larger channel gain region. The reason is that the probability that the system works in the low velocity and large channel gain region is smaller so that the system needs to use more power to fully utilize this region, especially for larger delay.

In Fig. 6, the ASE variation is shown as a function of SNR for different (μ, σ_v^2) values under perfect and imperfect cases. The figure also shows that there are differences in performance for different μ and σ_v^2 values. It can be observed from Fig. 6 that the proposed scheme is better than the traditional adaptation [8] and the mobility adaptation [13] for all

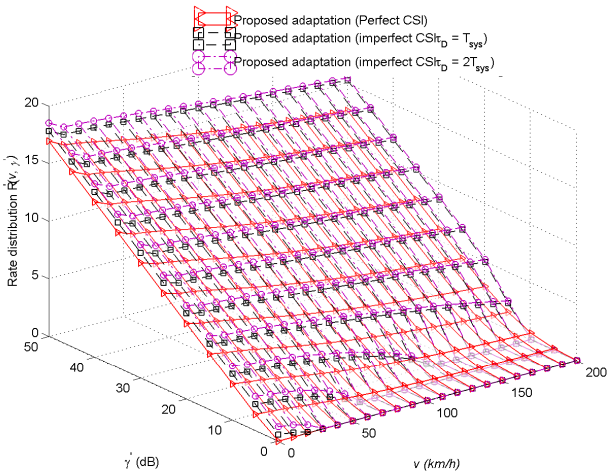

FIGURE 5. The rate distribution vs. velocity v and channel gain γ' under imperfect CSI case ($\mu = 150$ km/h, $\sigma_v^2 = 45$ (km/h)^2, SNR = 15 dB).

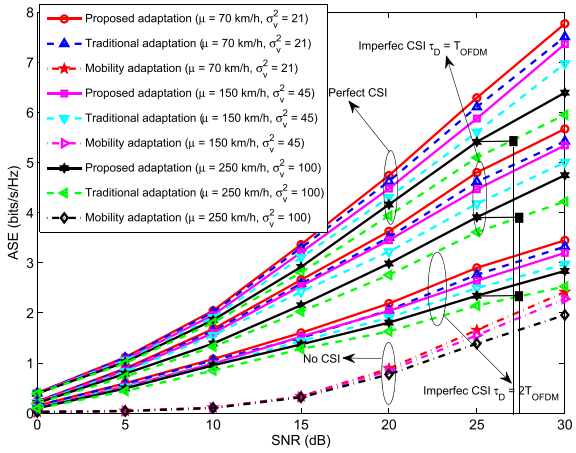

FIGURE 6. ASE vs. SNR.

SNRs. The performance decreases as the delay or the mean of velocity increases. We can observe that when delay is equal to $2T_{OFDM}$, we reach to a worst performance, compared with the case in which delay is equal to T_{OFDM} or the perfect CSI is achieved. Obviously, the proposed adaptation is closed to the mobility adaptation as the delay increases and when μ is fixed. From Fig. 6, we observe that the performance of ($\mu = 250$ km/h, $\sigma_v^2 = 100$ (km/h)^2) is worse than that of ($\mu = 150$ km/h , $\sigma_v^2 = 45$ (km/h)^2) and ($\mu = 70$ km/h, $\sigma_v^2 = 21$ (km/h)^2) due to the fact that the probability of the terminal velocities being in the high velocity region gets smaller for smaller values of μ. For example the probability of high velocity ranges ([200-300] km/h) for ($\mu = 250$ km/h, $\sigma_v^2 = 100$ (km/h)^2), ([200 − 300] km/h) for ($\mu = 150$ km/h, $\sigma_v^2 = 45$ (km/h)^2) and ([200 − 300] km/h) for ($\mu = 70$ km/h, $\sigma_v^2 = 21$ (km/h)^2) are 0.559, 0.133 and 3.00028×10^{-10}), respectively.

Consequently, the larger probability being in the high velocity region would lead to worse channel estimation error with the MMSE channel estimation method. In summary, it is obvious that the performance of proposed adaptation is close to mobility adaptation with μ increases because the worse channel estimation error will result in a very limited system performance based on imperfect CSI. Compared with traditional adaptation based on CSI only, the improvement of proposed adaptation is determined by μ and σ_v^2. The improvement increases as σ_v^2 increases because velocity variation increases with σ_v^2 increases. More specifically, the improvement between the proposed scheme with ($\mu = 250$ km/h, $\sigma_v^2 = 100$ (km/h)^2) and the traditional adaptation with ($\mu = 250$ km/h, $\sigma_v^2 = 100$ (km/h)^2) is about 2 *dB* which is quite significant as seen from Fig. 6. However, when the velocity variation is small, the improvement in performance between the proposed scheme with ($\mu = 70$ km/h, $\sigma_v^2 = 21$ (km/h)^2) and the traditional adaptation with ($\mu = 70$ km/h, $\sigma_v^2 = 21$ (km/h)^2) would be limited, especially when SNR is low.

VI. CONCLUSION

Due to the time-varying nature of doubly selective wireless channels, the performance of system is determined not only by the CSI, but also by the terminal velocities. The proposed power and rate adaptation by adjusting perfect and imperfect CSI and velocity is an effective way to improve the average spectral efficiency. The proposed scheme always chooses the better strategy (lower velocity and larger channel gain) to improve the system performance. The improvement of the proposed scheme, compared with traditional adaptation without knowing the prior knowledge of velocity and mobility adaptation without CSI, is quite effective.

Not surprisingly, the proposed adaptive scheme, which is based on velocity and CSI, is proposed with different mobility scenarios. For the stationary or low mobility, the proposed adaptive scheme is close to the traditional adaptive scheme based on CSI only because the improvement from velocity variation is limited. Therefore, if the terminal is stationary or moving very slowly such as indoor or pedestrian, then the traditional adaptation scheme based on the estimated CSI only could be chosen because of lower complexity. However, for the high mobility case, the proposed adaptive scheme is closed to the mobility adaptive scheme based on the velocity only because the improvement from CSI variations is also limited due to the imperfect CSI (channel estimation error and delay). On the other hand, if the velocity of terminal is very large such as high speed train, the traditional adaptation schemes based on CSI would be inefficient and yield poor performance results since the estimated CSI is not usable. Hence the mobility adaptation based on the velocity only should be adapted because of the lower complexity. Finally, if the velocity of terminal is in the intermediate region such as the velocities of urban and suburban vehicles, the proposed adaptation based on velocity and imperfect CSI should be employed in an efficient way.

APPENDIX A

In this appendix we prove that Eq. (12a) is concave with respect to $P(v, \gamma)$.

From (12a), define

$$C_{(v,\gamma)}(P(v,\gamma)) = \log_2\left[\frac{\xi\gamma P(v,\gamma)}{P_N\overline{\gamma}P(v,\gamma)+1}+1\right].$$

First order derivative of $C_{(v,\gamma)}(P(v,\gamma))$ with respect to $P(v,\gamma)$ can be obtained as

$$\frac{\partial C_{(v,\gamma)}(P(v,\gamma))}{\partial P(v,\gamma)} = \frac{\xi\gamma}{(\varsigma\varphi\ln(2))} > 0, \tag{30}$$

where $\varsigma = (P_N\overline{\gamma}P(v,\gamma)+1) > 0$, $\varphi = (\xi\gamma P(v,\gamma) + P_N\overline{\gamma}P(v,\gamma)+1) > 0$, $P(v,\gamma) \geq 0$ in (12c) and $\xi > 0$ with the target BER $C_3 = 10^{-3}$ in (10).

Similarly, second order derivative of $C_{(v,\gamma)}(P(v,\gamma))$ with respect to $P(v,\gamma)$ is

$$\frac{\partial^2 C_{(v,\gamma)}(P(v,\gamma))}{\partial P^2(v,\gamma)} = -\frac{\chi}{\left(\varsigma^2\varphi^2\ln(2)\right)} < 0, \tag{31}$$

where $\chi = (2\xi\gamma P(v,\gamma)P_N\overline{\gamma}+2P_N^2\overline{\gamma}^2P(v,\gamma)+2P_N\overline{\gamma}+\xi\gamma)\,\xi\gamma > 0$.

Based on **Second-order conditions** on [23, p. 71], it can easily follows from (31) that $C_{(v,\gamma)}(P(v,\gamma))$ is concave with respect to $P(v,\gamma)$.

Finally, based on **"Integrals of concave functions is concave"** on [23, p. 79], it can be shown that

$$\int_{v_{\min}}^{v_{\max}}\int_0^{\infty}\log_2\left[\frac{\xi\gamma P(v,\gamma)}{P_N\overline{\gamma}P(v,\gamma)+1}+1\right]p_\gamma(\gamma)f(v)d\gamma dv$$

is concave with respect to $P(v,\gamma)$.

APPENDIX B

In this appendix we prove that Eq. (12b) is affine with respect to $P(v,\gamma)$.

From (12c), based on **"Any line is affine"** on [23, p. 27], we can obtain that **dom** $P(v,\gamma)$ is a convex set (Here $P(v,\gamma)$ is a function of v and γ, we can still regard of $P(v,\gamma)$ as a whole).

For all $x, y \in$ **dom** $P(v,\gamma)$, and θ with $0 \leq \theta \leq 1$, we can obtain (32), as shown at the bottom of this page.

Therefore, based on **"A function is linear, *i.e.*, satisfy $f_i(\alpha x+\beta y) = \alpha f_i(x)+\beta f_i(y)$ for all $x, y \in R^n$ and all $\alpha, \beta \in R$."** on [23, p. 1], $\int_{v_{\min}}^{v_{\max}}\int_0^{\infty}P(v,\gamma)p_\gamma(\gamma)f(v)d\gamma dv - 1$ is a linear function with regards to $P(v,\gamma)$.

Based on **"Function always have equality in $f_i(\alpha x+\beta y) = \alpha f_i(x)+\beta f_i(x)$, linear functions are both convex and concave."** on [23, p. 67], the function $\int_{v_{\min}}^{v_{\max}}\int_0^{\infty}P(v,\gamma)p_\gamma(\gamma)f(v)d\gamma dv - 1$ is both convex and concave with respect to $P(v,\gamma)$.

Finally, based on **"any function that is convex and concave is affine"** on [23, p. 67], (12b) is affine with respect to $P(v,\gamma)$ [23].

APPENDIX C

In this appendix we prove that ϑ acts as a slack variable. Based on (13), we obtain the KKT conditions

$$\int_{v_{\min}}^{v_{\max}}\int_0^{\infty}P^*(v,\gamma)p_\gamma(\gamma)f(v)d\gamma dv = 1, \tag{33a}$$

$$P^*(v,\gamma) \geq 0, \tag{33b}$$

$$\vartheta^* \geq 0, \tag{33c}$$

$$\vartheta^*P^*(v,\gamma) = 0, \tag{33d}$$

$$\int_{v_{\min}}^{v_{\max}}\int_0^{\infty} \times\frac{\xi\gamma}{\ln(2)\,(P_N\overline{\gamma}P^*(v,\gamma)+1)\,(\xi\gamma P^*(v,\gamma)+P_N\overline{\gamma}P^*(v,\gamma)+1)} \times p_\gamma(\gamma)f(v)d\gamma dv - \lambda^*\int_{v_{\min}}^{v_{\max}}\int_0^{\infty}p_\gamma(\gamma)f(v)d\gamma dv - \vartheta^* = 0. \tag{33e}$$

These equations can be solved directly to find $P^*(v,\gamma)$, λ^* and ϑ^*, as follows. We start by noting that ϑ^* acts as a slack variable in the last equation, so it can be eliminated. Based on (33e), we can obtain (33f), as shown at the top of the next page. Substituting (33f) into (33a), (33b), (33c) and (33d) yields

$$\int_{v_{\min}}^{v_{\max}}\int_0^{\infty}P^*(v,\gamma)p_\gamma(\gamma)f(v)d\gamma dv = 1, \tag{33g}$$

$$P^*(v,\gamma) \geq 0, \tag{33h}$$

$$\int_{v_{\min}}^{v_{\max}}\int_0^{\infty} \times\frac{\xi\gamma}{\ln(2)\,(P_N\overline{\gamma}P^*(v,\gamma)+1)\,(\xi\gamma P^*(v,\gamma)+P_N\overline{\gamma}P^*(v,\gamma)+1)} \times p_\gamma(\gamma)f(v)d\gamma dv - \lambda^*\int_{v_{\min}}^{v_{\max}}\int_0^{\infty}p_\gamma(\gamma)f(v)d\gamma dv \geq 0 \tag{33i}$$

$$\left(\int_{v_{\min}}^{v_{\max}}\int_0^{\infty} \times\frac{\xi\gamma}{\ln(2)\,(P_N\overline{\gamma}P^*(v,\gamma)+1)\,(\xi\gamma P^*(v,\gamma)+P_N\overline{\gamma}P^*(v,\gamma)+1)} \times p_\gamma(\gamma)f(v)d\gamma dv - \lambda^*\int_{v_{\min}}^{v_{\max}}\int_0^{\infty}p_\gamma(\gamma)f(v)d\gamma dv\right) \times P^*(v,\gamma) = 0. \tag{33j}$$

$$\int_{v_{\min}}^{v_{\max}}\int_0^{\infty}(\theta x+(1-\theta)y)p_\gamma(\gamma)f(v)d\gamma dv - 1 = \theta\left(\int_{v_{\min}}^{v_{\max}}\int_0^{\infty}(x)p_\gamma(\gamma)f(v)d\gamma dv - 1\right) + (1-\theta)\left(\int_{v_{\min}}^{v_{\max}}\int_0^{\infty}(y)p_\gamma(\gamma)f(v)d\gamma dv - 1\right). \tag{32}$$

$$\vartheta^* = \int_{v_{\min}}^{v_{\max}} \int_0^{\infty} \frac{\xi\gamma}{\ln(2)\left(P_N\overline{\gamma}P^*(v,\gamma)+1\right)\left(\xi\gamma P^*(v,\gamma)+P_N\overline{\gamma}P^*(v,\gamma)+1\right)} p_\gamma(\gamma) f(v) d\gamma dv - \lambda^* \int_{v_{\min}}^{v_{\max}} \int_0^{\infty} p_\gamma(\gamma) f(v) d\gamma dv. \tag{33f}$$

$$C_{(v,\gamma')}(P'(v,\gamma')) = \log_2\left[\frac{B_1\left(\phi P'\left(v,\gamma'\right)+1\right)+B_4P'\left(v,\gamma'\right)W\left(B_3\right)-\sigma^2W\left(B_3\right)\left(\phi P'\left(v,\gamma'\right)+1\right)}{\left(B_1-\sigma^2W\left(B_3\right)\right)\left(\phi P'\left(v,\gamma'\right)+1\right)}\right], \tag{34}$$

$$\frac{\partial C_{(v,\gamma')}(P'(v,\gamma'))}{\partial P'(v,\gamma')} = \frac{B_4W(B_3)}{(\phi P'(v,\gamma')+1)((B_1-\sigma^2W(B_3))\phi P'(v,\gamma')+B_4P'(v,\gamma')W(B_3)+B_1-\sigma^2W(B_3))\ln(2)} > 0. \tag{37}$$

$$\frac{\partial^2 C_{(v,\gamma')}(P'(v,\gamma'))}{\partial P'^2(v,\gamma')} = -\frac{(B_4W(B_3))(2(B_1-\sigma^2W(B_3))\phi^2P'(v,\gamma')+2(B_1-\sigma^2W(B_3))\phi+2\phi B_4P'(v,\gamma')W(B_3)+B_4W(B_3))}{(\phi P'(v,\gamma')+1)^2(B_1\phi P'(v,\gamma')+B_1+B_4P'(v,\gamma')W(B_3)-\sigma^2W(B_3)\phi P'(v,\gamma')-\sigma^2W(B_3))^2\ln(2)} < 0. \tag{38}$$

"$\geq$0" can be considered as "$>$0" or "$=$0". Based on (33i), we can obtain

$$\int_{v_{\min}}^{v_{\max}} \int_0^{\infty} \times \frac{\xi\gamma}{\ln(2)(P_N\overline{\gamma}P^*(v,\gamma)+1)(\xi\gamma P^*(v,\gamma)+P_N\overline{\gamma}P^*(v,\gamma)+1)} \times p_\gamma(\gamma)f(v)d\gamma dv > \lambda^* \int_{v_{\min}}^{v_{\max}} \int_0^{\infty} p_\gamma(\gamma)f(v)d\gamma dv,$$

or

$$\int_{v_{\min}}^{v_{\max}} \int_0^{\infty} \times \frac{\xi\gamma}{\ln(2)(P_N\overline{\gamma}P^*(v,\gamma)+1)(\xi\gamma P^*(v,\gamma)+P_N\overline{\gamma}P^*(v,\gamma)+1)} \times p_\gamma(\gamma)f(v)d\gamma dv = \lambda^* \int_{v_{\min}}^{v_{\max}} \int_0^{\infty} p_\gamma(\gamma)f(v)d\gamma dv.$$

Then, if "$>$" holds in the above, based on (33j), we can get $P^*(v,\gamma)=0$, implying that there is no data transmission since no power allocation could be made. On the other hand, if "$=$" holds, based on (33h), we can obtain $P^*(v,\gamma)\geq 0$. When $P^*(v,\gamma)=0$, there exists a cutoff value, below which no data is transmitted and in this case, based on (33f), as show at the top of this page, it follows that $\vartheta^*=0$. Therefore, ϑ^* acts as a slack variable and it can be eliminated.

APPENDIX D

In this appendix we prove that (26a) is concave with respect to $P'\left(v,\gamma'\right)$.

From (26a), we define (34), as shown at the top of this page, where $B_1 = \frac{r^2\gamma'}{\left(\rho_0+\sigma_p^2/N\right)^2\overline{\gamma}} > 0$, $B_3 = \frac{B_1C_3\exp\left(B_1/\sigma^2\right)}{C_1\sigma^2} > 0$, $B_4 = C_2\overline{\gamma}\sigma^4 > 0$ in (24), $\phi > 0$ in (20) and $\sigma^2 > 0$ in (23). $W(.)$ denotes the Lambert W function that satisfies $W(x)\exp\left(W(x)\right)=x$, as shown in [30]. The related properties are as follows: ①. $W(x)$ is an increasing function when $x\geq 0$ [30]. ②. The following can be obtained easily

$$W\left(ax\exp\left(x\right)\right) < W\left(x\exp\left(x\right)\right) = x \tag{35}$$

when $x\geq 0$ and $0<a<1$.

Set $a=\frac{C_3}{C_1}$ and $x=\left(B_1/\sigma^2\right)$ for B_3. Based on (35), we can obtain

$$W(B_3) < B_1/\sigma^2 \tag{36}$$

where $C_1 = 0.2$ in (9), the target BER C_3 is 10^{-3} and $0<\frac{C_3}{C_1}<1$.

First order derivative of $C_{(v,\gamma')}$ with respect to $P'(v,\gamma')$ is obtained as in (37), as shown at the top of this page.

The second order derivative of $C_{(v,\gamma')}$ with respect to $P'(v,\gamma')$ is obtained as in (38), as shown at the top of this page.

Therefore, based on **Second-order conditions** on [23, p. 71], $C_{(v,\gamma')}(P'(v,\gamma'))$ is concave with respect to $P'(v,\gamma')$.

Finally, based on **"Integrals of concave functions is concave"** on [23, p. 79], it is obtained that (26a) is concave with respect to $P'\left(v,\gamma'\right)$.

ACKNOWLEDGMENTS

The authors would like to thank the anonymous reviewers for their comments and suggestions, which helped improving significantly the quality of the manuscript.

REFERENCES

[1] R. Prasad, *OFDM for Wireless Communications Systems*. Norwood, MA, USA: Artech House, 2004.

[2] Y. Li and L. J. Cimini, "Bounds on the interchannel interference of OFDM in time-varying impairments," *IEEE Trans. Commun.*, vol. 49, no. 3, pp. 401–404, Mar. 2001.
[3] X. Cai and G. B. Giannakis, "Bounding performance and suppressing intercarrier interference in wireless mobile OFDM," *IEEE Trans. Commun.*, vol. 51, no. 12, pp. 2047–2056, Dec. 2003.
[4] A. J. Goldsmith and S.-G. Chua, "Variable-rate variable-power MQAM for fading channels," *IEEE Trans. Commun.*, vol. 45, no. 10, pp. 1218–1230, Oct. 1997.
[5] E. Bedeer, O. A. Dobre, M. H. Ahmed, and K. E. Baddour, "A systematic approach to jointly optimize rate and power consumption for OFDM systems," *IEEE Trans. Mobile Comput.*, vol. 15, no. 6, pp. 1305–1317, Jun. 2016.
[6] H. Holma and A. Toskala, *HSDPA/HSUPA for UMTS: High Speed Radio Access for Mobile Communication*. New York, NY, USA: Wiley, 2007.
[7] Y. Saito, Y. Kishiyama, A. Benjebbour, T. Nakamura, A. Li, and K. Higuchi, "Non-orthogonal multiple access (NOMA) for cellular future radio access," in *Proc. IEEE 77th Veh. Technol. Conf.*, Jun. 2013, pp. 1–5.
[8] Z. Dong, P. Fan, E. Panayirci, and P. T. Mathiopoulos, "Effect of power and rate adaptation on the spectral efficiency of MQAM/OFDM system under very fast fading channels," *EURASIP J. Wireless Commun. Network.*, vol. 2012, no. 1, pp. 1–15, Jul. 2012.
[9] Z. Dong, P. Fan, W. Zhou, and E. Panayirci, "Power and rate adaptation for MQAM/OFDM systems under fast fading channels," in *Proc. IEEE 75th Veh. Technol. Conf. (VTC Spring)*, May 2012, pp. 1–5.
[10] S. S. Das, E. D. Carvalho, and R. Prasad, "Performance analysis of OFDM systems with adaptive sub carrier bandwidth," *IEEE Trans. Wireless Commun.*, vol. 7, no. 4, pp. 1117–1122, Apr. 2008.
[11] J. Wen, C. Chiang, T. Hsu, and H. Hung, "Resource management techniques for OFDM systems with the presence of inter-carrier interference," *Wireless Pers. Commun.*, vol. 65, no. 3, pp. 515–535, Aug. 2012.
[12] Z. Dong, P. Fan, and X. Lei, "Mobility adaptation in OFDM systems over rapidly time-varying fading channels," in *Proc. IEEE Int. Conf. Commun. Syst. (ICCS)*, Nov. 2014, pp. 318–322.
[13] Z. Dong, P. Fan, and X. Lei, "Power adaptation in OFDM systems based on velocity variation under rapidly time-varying channels," *IEEE Commun. Lett.*, vol. 19, no. 4, pp. 689–692, Apr. 2015.
[14] S. Yousefi, E. Altman, R. El-Azouzi, and M. Fathy, "Analytical model for connectivity in vehicular ad hoc networks," *IEEE Trans. Veh. Technol.*, vol. 57, no. 6, pp. 3341–3356, Nov. 2008.
[15] S. Mohanty, "VEPSD: A novel velocity estimation algorithm for next-generation wireless systems," *IEEE Trans. Wireless Commun.*, vol. 4, no. 6, pp. 2655–2660, Nov. 2005.
[16] W. Lee and D.-H. Cho, "Mean velocity estimation of mobile stations by spatial correlation of channels in cellular systems," *IEEE Commun. Lett.*, vol. 13, no. 9, pp. 670–672, Sep. 2009.
[17] E. Panayirci, H. Senol, and H. V. Poor, "Joint channel estimation, equalization, and data detection for OFDM systems in the presence of very high mobility," *IEEE Trans. Signal Process.*, vol. 58, no. 8, pp. 4225–4238, Aug. 2010.
[18] O. B. Karimi, J. Liu, and C. Wang, "Seamless wireless connectivity for multimedia services in high speed trains," *IEEE J. Sel. Areas Commun.*, vol. 30, no. 4, pp. 729–739, May 2012.
[19] Y.-S. Choi, P. J. Voltz, and F. A. Cassara, "On channel estimation and detection for multicarrier signals in fast and selective Rayleigh fading channels," *IEEE Trans. Commun.*, vol. 49, no. 8, pp. 1375–1387, Aug. 2001.
[20] S. Ye, R. Blum, and L. Cimini, "Adaptive OFDM systems with imperfect channel state information," *IEEE Trans. Wireless Commun.*, vol. 5, no. 11, pp. 3255–3265, Nov. 2006.
[21] Z. Dong, P. Fan, E. Panayirci, and X. Lei, "Conditional power and rate adaptation for MQAM/OFDM systems under CFO with perfect and imperfect channel estimation errors," *IEEE Trans. Veh. Technol.*, vol. 64, no. 11, pp. 5042–5055, Nov. 2015.
[22] S. T. Chung and A. J. Goldsmith, "Degrees of freedom in adaptive modulation: A unified view," *IEEE Trans. Commun.*, vol. 49, no. 9, pp. 1561–1571, Sep. 2001.
[23] S. Boyd and L. Vandenberghe, *Convex Optimization*. Cambridge, U.K.: Cambridge Univ. Press, 2004.
[24] C. S. Tocci and S. Adams, *Applied Maple for Engineers and Scientists*. Norwood, MA, USA: Artech House, 1996.
[25] T. Gucluoglu and E. Panayirci, "Performance of transmit and receive antenna selection in the presence of channel estimation errors," *IEEE Commun. Lett.*, vol. 12, no. 5, pp. 371–373, May 2008.
[26] E. Basar, U. Aygolu, E. Panayirci, and H. V. Poor, "Performance of spatial modulation in the presence of channel estimation errors," *IEEE Commun. Lett.*, vol. 16, no. 2, pp. 176–179, Feb. 2012.
[27] Z. Dong, P. Fan, R. Q. Hu, J. Gunther, and X. Lei, "On the spectral efficiency of rate and subcarrier bandwidth adaptive OFDM systems over very fast fading channels," *IEEE Trans. Veh. Technol.*, vol. 65, no. 8, pp. 6038–6050, Aug. 2016.
[28] E. Panayirci, H. Dogan, and H. V. Poor, "Low-complexity map-based successive data detection for coded OFDM systems over highly mobile wireless channels," *IEEE Trans. Veh. Technol.*, vol. 60, no. 6, pp. 2849–2857, Jul. 2011.
[29] N. Sun and J. Wu, "Maximizing spectral efficiency for high mobility systems with imperfect channel state information," *IEEE Trans. Wireless Commun.*, vol. 13, no. 3, pp. 1462–1470, Mar. 2014.
[30] R. M. Corless, G. H. Gonnet, D. E. Hare, D. J. Jeffrey, and D. E. Knuth, "Lambert W function in Maple," *Maple Tech. Newslett.*, vol. 9, pp. 12–22, 1993.
[31] 3GPP, "3rd generation partnership project; technical specification group radio access network; feasibility study for orthogonal frequency division multiplexing (OFDM) for UTRAN enhancement (Release 6)," Tech. Rep. TR 25.892 V6.0.0 (2004-06), Jun. 2004, pp. 1–91.

ZHI-CHENG DONG (SM'12–M'16) was born in Langzhong, China, in 1982. He received the B.E., M.S., and Ph.D. degrees from the School of Information Science and Technology, Southwest Jiaotong University, Chengdu, China, in 2004, 2008, and 2016, respectively. Since 2016, he has been an Associate Professor with the School of Engineering, Tibet University, Lhasa, China. He has served as a Technical Program Committee Member of the IEEE Globecom 2017, the IEEE ICC in 2015, 2016, and 2017, the IEEE TENSYMP in 2015, and Chinacom in 2014.

His current research interests include adaptation technology, performance analysis, and signal processing for high mobility wireless communications.

PING-ZHI FAN (M'93–SM'99–F'15) received the Ph.D. degree in electronic engineering from Hull University, U.K. He is currently a Professor and the Director of the Institute of Mobile Communications, Southwest Jiaotong University, China. He is also the IEEE VTS Distinguished Lecturer. He has authored over 200 research papers in various academic English journals, and eight books (including edited) authored by John Wiley & Sons Ltd/RSP. His current research interests include high mobility wireless communications, wireless networks for big data, 5G technologies, and signal design and coding. He is a recipient of the UK ORS Award and the NSFC Outstanding Young Scientist Award, and the Chief Scientist of a National 973 Major Research Project. He is a fellow of the IET(IEE), the CIC, and the CIE.

XIAN-FU LEI (M'14) was born in 1981. He received the Ph.D. degree in communication and information system from Southwest Jiaotong University in 2012. From 2012 to 2014, he was a Research Fellow with the Department of Electrical and Computer Engineering, Utah State University, USA. Since 2015, he has been an Associate Professor with the School of Information Science and Technology, Southwest Jiaotong University, China. He has authored nearly 70 journal and conference papers on these topics. His current research interests include 5G wireless communications, cooperative communications, cognitive radio, physical layer security, and energy harvesting. He received an Exemplary Reviewer Certificate of the IEEE COMMUNICATIONS LETTERS and an Exemplary Reviewer Certificate of the IEEE WIRELESS COMMUNICATIONS LETTERS in 2013. He currently serves on the Editorial Board of the IEEE COMMUNICATIONS LETTERS, the IEEE ACCESS, the *Wireless Communications and Mobile Computing*, the *Security and Communication Networks*, the *KSII Transactions on Internet and Information Systems*, and the *Telecommunication Systems*. He has served as a Guest Editor of the Special Issue of the Non-Orthogonal Multiple Access for 5G Systems in the IEEE JOURNAL ON SELECTED AREAS IN COMMUNICATIONS in 2016 and the Lead Guest Editor of the Special Issue of the Energy Harvesting Wireless Communications in the *EURASIP Journal on Wireless Communications and Networking* in 2014. He has also served as a TPC member for major international conferences, such as the IEEE ICC, the IEEE GLOBECOM, the IEEE WCNC, the IEEE VTC Spring/Fall, and the IEEE PIMRC.

ERDAL-PANAYIRCI (M'80–SM'91–F'03–LF'06) received the Diploma Engineering degree in electrical engineering from Istanbul Technical University, Istanbul, Turkey, and the Ph.D. degree in electrical engineering and system science from Michigan State University, USA. Until 1998, he was with the Faculty of Electrical and Electronics Engineering, Istanbul Technical University, where he was a Professor and the Head of the Telecommunications Chair. He spent the academic year 2008–2009 with the Department of Electrical Engineering, Princeton University, NJ, USA, where he was involved in new channel estimation and equalization algorithms for high mobility WIMAX and LTE systems. He is currently a Professor of Electrical Engineering and the Head of the Electronics Engineering Department, Kadir Has University, Istanbul. He has been the Principal Coordinator of the sixth and seventh Frame European project called Network of Excellent on Wireless Communications representing Kadir Has University for five years and WIMAGIC Strep project for two years. He has authored extensively in leading scientific journals and international conference and co-authored the book *Principles of Integrated Maritime Surveillance Systems* (Boston, Kluwer Academic Publishers, 2000). His current research interests include communication theory, synchronization, applications of the advanced signal processing techniques to electrical, optical, and underwater acoustic wireless communications. He served as a member of IEEE Fellow Committee from 2005 to 2008. He was the Technical Program Co-Chair of the IEEE International Conference on Communications and the Technical Program Chair of the IEEE PIMRC, Istanbul, Turkey, in 2006 and 2010, respectively. He was an Editor of the IEEE TRANSACTIONS ON COMMUNICATIONS in synchronization and equalizations in 1995–1999. He is the Executive Vice Chairman of the IEEE Wireless Communications and Networking Conference, Istanbul, in 2014. He is currently the Head of the Turkish Scientific Commission on Signals and Systems of URSI.